Multipath interferometer with ultracold atoms trapped in an optical lattice

J. Chwedeńczuk,[1] F. Piazza,[2] and A. Smerzi[3]

[1]*Faculty of Physics, University of Warsaw, ul. Hoża 69, PL-00-681 Warszawa, Poland*

[2]*Physik Department, Technische Universität München, D-85747 Garching, Germany*

[3]*QSTAR Center for Quantum Science and Technology, CNR-INO and LENS, Largo Enrico Fermi 2, I-50125 Arcetri, Italy*

We study an ultracold gas of N bosons trapped in a one-dimensional M-site optical lattice perturbed by a spatially dependent potential gx^j, where the unknown coupling strength g is to be estimated. We find that the measurement uncertainty is bounded by $\Delta g \propto \frac{1}{N(M^j - 1)}$. For a typical case of a linear potential, the sensitivity improves as M^{-1}, which is a result of multiple interferences between the sites, an advantage of multipath interferometers over two-mode setups. Next, we calculate the estimation sensitivity for a specific measurement where, after the action of the potential, the particles are released from the lattice and form an interference pattern. If the parameter is estimated by a least-squares fit of the average density to the interference pattern, the sensitivity still scales like M^{-1} for linear potentials. We finally discuss the role of useful entanglement of the initial state in the lattice to beat the shot-noise limit.

PACS number(s): 03.75.Dg, 37.25.+k, 03.75.Gg

I. INTRODUCTION

As scientists gain insight into the microscale in both the space and time domains, it becomes increasingly relevant to develop ultraprecise measurement devices. Very prominent among those are interferometers, where the parameter to be measured is mapped into a phase difference θ (or optical path length difference) between two (or more) arms of the device. By recombining the outputs of each arm, an interference figure appears, which contains information about the parameter to be estimated.

The key quantity which describes the performance of an interferometer is its sensitivity. In a typical interferometer, where the signal which is used to determine θ comes from a collection of N independent particles, the precision scales at the shot-noise level, i.e., $\Delta\theta \propto \frac{1}{\sqrt{m}} \frac{1}{\sqrt{N}}$, where m denotes the number of independent repetitions of the measurement. This expression tells us that the sensitivity can be improved by either increasing the number of trials m or the number of probe particles N. A third way of decreasing $\Delta\theta$ is by replacing the uncorrelated ensemble of atoms with a usefully entangled state. Nonclassical correlations can be employed to beat the shot-noise limit (SNL) and ultimately reach the Heisenberg limit (HL), where $\Delta\theta \propto \frac{1}{\sqrt{m}} \frac{1}{N}$, which for large N can be a significant improvement over the SNL [1–3].

A paradigmatic example of an interferometer which benefits from the use of entangled states is a Mach-Zehnder interferometer (MZI), where the signal coming from two arms at the input is first split using a beam splitter, then the phase difference is imprinted between the two arms, and finally, another beam splitter maps the phase difference into the intensities in the output ports. When the MZI is fed with a useful-entangled state [3] and the phase θ is estimated from the measurement of the population imbalance between these ports, it is possible to achieve a sub-shot-noise (SSN) sensitivity $\Delta\theta < \frac{1}{\sqrt{m}} \frac{1}{\sqrt{N}}$.

While originally implemented with photons, in recent years interferometers fed by atoms have attracted much interest [4] and will be the subject of the present work. These interferometers proved promising for the precise determination of electromagnetic [5–7] and gravitational [8–10] interactions. Moreover, their performance can be improved with the recently created nonclassical states of matter [11–16] by squeezing the atom number fluctuations between two modes while keeping high mutual coherence. In [13], such a spin-squeezed state was generated in an external double-well potential, while in [14–18] internal degrees of freedom were employed. In the experiments mentioned above, a two-path (or two-mode) usefully entangled quantum state was prepared. In this work, we consider instead a multipath atom interferometer, involving more than two internal or external degrees of freedom.

The idea that the growing number of modes could improve the performance of an interferometer was first discussed in the context of optical devices [19,20]. They involve the multimode version of a beam splitter and allow us, in general, to measure a vector phase [21]. In the particular case where the phase difference is the same between each pair of "neighboring" paths, different methods have been used to derive bounds for the phase sensitivity. In [20], for an input coherent state, the error-propagation formula allowed to predict a sensitivity $\Delta\theta \propto M^{-1}$, where M is the number of ports. This is a result of a multiple interference between different paths and does not violate the HL [22]. The gain is also robust against losses [20], differently from the improvement due to entanglement present in the input state. The scaling of the sensitivity with the number of modes and particles has also been heuristically derived for the specific case where coherent or number states are used as input [23]. Recently, the sensitivity of rotation measurements using a ring interferometer with ultracold atoms inside a lattice has been studied in [24]. Numerical determination of the ground state allowed to calculate the quantum Fisher information (QFI) for specific states, which, as we will discuss in the following, provides the ultimate sensitivity bound, independently of the measurement and estimation strategy employed.

On the experimental side, multimode atom interferometry has been applied in the context of gravitometry by implementing multiple-wave quantum levitators [25]. With these devices, the improvement of the measurement sensitivity due to multiple-wave interferences has been demonstrated by applying successive momentum transfer pulses on a free-falling

Bose-Einstein condensate [26]. Another implementation with Bose-Einstein condensates has been realized recently in [27] and involves splitting among internal Zeeman sublevels. In this case, an increased interferometric signal, with respect to the two-mode case, was observed, which is the main effect analyzed in our work. In a stationary-wave optical lattice, the improvement of the measurement sensitivity using Bloch oscillations has been demonstrated in [28] by dynamically delocalizing the atomic wave function over a large number of lattice sites [29,30]. A first step towards realizing a quantum multipath interferometer has been recently made by creating a multimode nonclassical state of ultracold bosons inside an optical lattice [31].

In this paper, we consider a multipath interferometer realized with a dilute gas of N ultracold bosons trapped inside a one-dimensional optical lattice [32–34]. Each of the M lattice sites plays the role of a possible interferometric path, whose optical length can be modified by adding a spatially dependent force which would be then the object of our precision measurement. More precisely, for a potential $V(x) = g\,x^j$, we derive the sensitivity for the estimation of the parameter g. First, using the quantum Fisher information (QFI) optimized over all possible input states, we show that the best possible precision is $\Delta g \propto \frac{1}{\sqrt{m}N(M^j-1)}$. Then, choosing a specific class of states which are symmetric with respect to the exchange of lattice sites, we obtain the sensitivity $\Delta g \propto \frac{1}{\sqrt{m}f(N)M^j}$ for $M \gg 1$. Here, $f(N)$ is the entanglement measure, which can vary from N for the superfluid state of the lattice up to N^2 for an entangled state. Note that when the potential $V(x)$ acts on the system, one can naturally define a phase $\theta = g x_0^j t/\hbar$, which is related to the coupling constant, the duration of the interaction t and the lattice spacing x_0. In the spirit of the two-mode interferometry, one can thus speak of the phase estimation, rather than determination of the coupling constant g. Throughout this work, we use both Δg and $\Delta \theta$ and keep in mind they are simply related by $\Delta g = (\hbar/t x_0^j)\Delta\theta$.

We finally consider a specific measurement and estimation strategy which could be applied in most of the current ultracold atom experimental setups: after undergoing the action of the force, the atoms are released from the lattice, form an interference pattern, and the parameter is extracted by a least-squares fit of the average density. Using rigorous results from the estimation theory [35], we derive the sensitivity for this interferometric protocol and show that it scales with M in the same way as in the case of the optimal measurement. The use of the spatial interference pattern, obtained through the expansion of the cloud, substitutes for the beam splitter. The *in situ* implementation of the latter in an optical lattice, in analogy to the double-well implementation, seems a much more demanding task.

This paper is organized as follows. In Sec. II we formulate the framework for analyzing the performance of the multimode interferometers. In Sec. III, we employ the notion of the QFI to provide some ultimate bounds for the multimode interferometry. First, in Sec. III A we identify the states which allow us to reach the best possible scaling of $\Delta\theta$ with the number of sites M and linear potentials $V(x) = gx$. Then in Sec. III B, using the QFI, we show how $\Delta\theta$ scales with M for states which are symmetric with respect to the interchange of any two sites. In Sec. III C we generalize these results for nonlinear

potentials $V(x) = gx^j$. Finally, in Sec. IV we show how the scaling with the number of sites can be achieved for a particular detection scheme and identify the states usefully entangled for the multimode interferometry. Some details of the analytical calculations are presented in the appendices.

II. FORMULATION OF THE MODEL

We begin the analysis of the multimode interferometry by introducing the quantum state $|\psi\rangle$ of N bosons distributed among M modes. The most general expression for $|\psi\rangle$ is

$$|\psi\rangle = \sum_{n_1=0}^{N} \sum_{n_2=0}^{N-n_1} \cdots \sum_{n_{M-1}=0}^{N-n_1-\cdots-n_{M-2}} C_{n_1\cdots n_{M-1}}$$
$$\times |n_1, n_2, \ldots, n_{M-1}, N - n_1 - \cdots - n_{M-1}\rangle, \quad (1)$$

where the sum runs over occupations of $M-1$ wells. Since the total number of atoms is set to be N, the population of the Mth mode is determined by other $M-1$ occupancies. The coefficient $C_{n_1\cdots n_{M-1}}$ is the probability amplitude for having $n_1 \cdots n_{M-1}$ atoms in the $M-1$ modes and $N - (n_1 + \cdots + n_{M-1})$ in the last one.

For future purposes we introduce a shortened notation, where the set of $M-1$ indices $(n_1 \cdots n_{M-1})$ is represented by a vector $\vec{n}$, and the state (1) is written as

$$|\psi\rangle = \sum_{\vec{n}} C_{\vec{n}} |\vec{n}\rangle. \quad (2)$$

The complete description of quantum properties of the system includes the M-mode field operator, which reads

$$\hat{\Psi}(x) = \sum_{k=1}^{M} \psi_k(x)\hat{a}_k. \quad (3)$$

Here, $\hat{a}_k$ is a bosonic operator which annihilates an atom occupying the mode function $\psi_k(x)$ localized in the kth well.

Let us for now restrict ourselves to the case where a constant force, corresponding to the linear potential $V(x) = gx$, is added to the lattice potential (the more general case will be consider in Sec. III C). Here g is the coupling constant, the parameter which we want to estimate.

The Hamiltonian corresponding to the added potential, in the second quantization, reads

$$\hat{H} = \epsilon \sum_{k=1}^{M} k\hat{n}_k, \quad (4)$$

where $\hat{n}_k = \hat{a}_k^\dagger \hat{a}_k$ is the on-site atom number operator and $\epsilon = gx_0$, where x_0 is the lattice spacing. The external force interacts with the trapped gas for a time t, which transforms the field operator (3) as follows:

$$\hat{\Psi}(x|\theta) \equiv e^{i\theta\hat{h}}\hat{\Psi}(x)e^{-i\theta\hat{h}} = \sum_{k=1}^{M} \psi_k(x)\hat{a}_k e^{-ik\theta}, \quad (5)$$

where $\theta = \epsilon t/\hbar$ and $\hat{h}$ is the generator of the phase-shift transformation,

$$\hat{h} = \sum_{k=1}^{M} k\hat{n}_k. \quad (6)$$

Equation (5) shows that the perturbation imprints a phase θ between two neighboring sites, while the phase between the two most distant wells is $(M-1)\theta$.

The interferometric sequence consists thus of a simple phase shift acting on the input state (2) and could be implemented as follows. First is the preparation of input state (2) in an unperturbed optical lattice ($g = 0$). Then the perturbing potential is suddenly turned on at a time scale shorter than the lattice hopping time, but slow enough to avoid creating higher band excitations. In this way, the state does not follow the change adiabatically, and the evolution operator is $\exp(-i\hat{h}\theta)$. The goal of this work is to derive the sensitivity of the estimation of θ or, equivalently, of the coupling constant $\Delta g = (\hbar/t x_0)\Delta\theta$.

Given the interferometric operation defined by Eqs. (5) and (6), the sensitivity $\Delta\theta$ still depends on (a) the choice of the *input state* $|\psi\rangle$, (b) the choice of the *measurement* to be performed on the final state $\exp(-i\hat{h}\theta)|\psi\rangle$, and (c) the choice of the *estimator*, that is, how to infer the value of the parameter given the measurement outputs. In Sec. III, we will derive the *optimal sensitivity*, that is, assuming that both the measurement and the estimator are the best achievable. This can be done using the notion of the QFI. The latter allows us to calculate the optimal sensitivity for a given input state. By further optimizing the QFI over all possible input states, one can derive the ultimate scaling of the sensitivity.

III. SENSITIVITY FOR THE OPTIMAL MEASUREMENT

A. Ultimate scaling

As anticipated, using the notion of the QFI, denoted here as F_Q, we can calculate the sensitivity for the best possible measurement and estimator. Once we know F_Q, we can indeed employ the Cramér-Rao lower bound (CRLB) [36]:

$$\Delta^2\theta \geqslant \frac{1}{m}\frac{1}{F_Q}, \tag{7}$$

where m is the number of independent repetitions of the measurement used to estimate θ. The right side of Eq. (7) is the sensitivity optimized over all possible measurements and estimators.

The QFI yet depends on the interferometric operation and the input state. For pure states, the value of F_Q is given by four times the variance of the generator of the interferometric operation $\hat{h}$, calculated with the input state,

$$F_Q = 4[\langle\psi|\hat{h}^2|\psi\rangle - \langle\psi|\hat{h}|\psi\rangle^2] \equiv 4\Delta^2\hat{h}. \tag{8}$$

The QFI can be maximized with respect to $|\psi\rangle$, and the upper bound for F_Q is provided by a simple relation [1]:

$$F_Q \leqslant (\lambda_{\max} - \lambda_{\min})^2, \tag{9}$$

where $\lambda_{\min,\max}$ are the smallest and largest eigenvalues of the operator $\hat{h}$. The two eigenvectors of $\hat{h}$ with extreme eigenvalues are

$$|\psi_{\min}\rangle = |N,0,\ldots,0\rangle \rightarrow \hat{h}|\psi_{\min}\rangle = N|\psi_{\min}\rangle, \tag{10a}$$

$$|\psi_{\max}\rangle = |0,0,\ldots,N\rangle \rightarrow \hat{h}|\psi_{\max}\rangle = MN|\psi_{\max}\rangle. \tag{10b}$$

By combining Eqs. (9) and (10) we get $F_Q \leqslant N^2(M-1)^2$. The inequality is saturated for the NOON state

$\frac{1}{\sqrt{2}}(|\psi_{\min}\rangle + |\psi_{\max}\rangle)$ for which, according to Eq. (7), the sensitivity is bounded by

$$\Delta^2\theta \geqslant \frac{1}{m}\frac{1}{N^2}\frac{1}{(M-1)^2}. \tag{11}$$

This expression is the first important result: when the perturbation is a linear potential (constant force), the best sensitivity reachable scales like M^{-1}, a kind of "Heisenberg scaling" with the number of wells. In Sec. III C, we will derive the equivalent bound for nonlinear potentials.

As anticipated in the Introduction, this scaling is a purely geometrical, and thus not quantum, effect. While the Heisenberg scaling with the number of atoms N originates from a macroscopic quantum superposition present in the NOON state, the scaling with M is a result of an accumulated phase shift between two extreme sites, as discussed below Eq. (6).

B. Scaling for symmetric states

Our next step is to remove the optimization of the QFI over all possible input states $|\psi\rangle$ and concentrate on a particular family of states which is more relevant for current experimental setups with ultracold atoms. We assume thus that N atoms are distributed among M sites symmetrically; i.e., the coefficient $C_{\vec{n}}$ is invariant upon the exchange of any two indices. A prominent member of such a family of states is the superfluid state [32], where each atom is in a coherent superposition, i.e.,

$$|\psi_{\mathrm{sf}}\rangle = \frac{1}{\sqrt{N!M^N}}(\hat{a}_1^\dagger + \cdots + \hat{a}_M^\dagger)^N|0\rangle. \tag{12}$$

This state can be written in form (2) with coefficients

$$C_{\vec{n}} = \frac{1}{\sqrt{M^N}}\frac{\sqrt{N!}}{\sqrt{n_1!\cdots n_{M-1}!(N-n_1-\cdots-n_{M-1})!}}, \tag{13}$$

which clearly possess the aforementioned symmetry. Another example is a symmetric Mott insulator state [32], where each site is occupied by $\frac{N}{M}$ atoms. Below we calculate the sensitivity $\Delta^2\theta$ using a generic symmetric state without taking any specific value of $C_{\vec{n}}$.

To this end, we calculate the QFI using Eq. (8) and the phase-transformation generator $\hat{h}$ for a linear perturbing potential from Eq. (6). The average is equal to

$$\langle\psi|\hat{h}|\psi\rangle = \sum_{k=1}^{M}k\langle\hat{n}_k\rangle = \frac{1}{2}(M+1)N, \tag{14}$$

where in the last step, due to the imposed symmetry, we used $\langle\hat{n}_k\rangle = \frac{N}{M}$. Calculating the average of $\hat{h}^2$ involves a few intermediate steps, which are presented in detail in Appendix A. The final result is that, for symmetric states and a linear perturbing potential, the QFI reads

$$F_Q = \tfrac{1}{3}(M+1)M^2\Delta^2\hat{n}, \tag{15}$$

where $\Delta^2\hat{n} = \langle\hat{n}^2\rangle - \langle\hat{n}\rangle^2$ is the on-site variance of the atom number. The value of $\Delta^2\hat{n}$ can be easily calculated for some particular states. For instance, the uncorrelated superfluid state (12) gives $\Delta^2\hat{n} = \frac{M-1}{M^2}N$, and as a consequence the QFI scales at the SNL, i.e., $F_Q = \frac{1}{3}(M^2-1)N$. A strongly entangled

symmetric NOON state [37]

$$|\psi_{\mathrm{NOON}}\rangle = \frac{|N,0,\ldots,0\rangle + |0,N,\ldots,0\rangle + \cdots + |0,\ldots,N\rangle}{\sqrt{M}}$$

$$(16)$$

gives $\Delta^2 \hat{n} = \frac{M-1}{M^2} N^2$, and as a consequence, the Heisenberg scaling of the QFI $F_Q = \frac{1}{3}(M^2 - 1)N^2$.

These two examples suggest that for all symmetric states the on-site variance has a particularly simple form $\Delta^2 \hat{n} = \frac{M-1}{M^2} f(N)$, where $f(N)$ does not depend on M. Indeed, the above form of $\Delta^2 \hat{n}$ can be explained as follows. When the "volume" of the system, in this case the number of sites M, tends to infinity, the atom number fluctuations in one site tend to zero. On the other hand, when the whole system consists of only one site, the fluctuations are zero since the number of atoms in the system is fixed. The only possible dependence of the variance on M, which behaves correctly in both these regimes and also accounts for the scaling of the average value, $\langle \hat{n} \rangle^2 = \frac{N^2}{M^2}$, is thus $\Delta^2 \hat{n} = \frac{M-1}{M^2} f(N)$. Putting this into Eq. (15) gives $F_Q = \frac{1}{3}(M^2 - 1)f(N)$ and the sensitivity

$$\Delta^2 \theta \geqslant \frac{1}{m} \frac{1}{f(N)} \frac{3}{M^2 - 1}. \tag{17}$$

The function $f(N)$ can be interpreted as a measure of the entanglement present in the system, related to the increased on-site atom number fluctuations. In the two-well case $M = 2$, such usefully entangled states which give $\Delta^2 \hat{n} > N$ are called "phase squeezed" [38] because the growth of the number fluctuations is accompanied by a decreased spread of the conjugate variable, which is the relative phase between the wells. Most important, the scaling with M of the sensitivity for symmetric states (17) is only slightly worse than the ultimate scaling (11) obtained for the best possible state and becomes the same for large M.

C. Scaling for nonlinear potentials

In this section, we generalize the results of Sec. III A for nonlinear potentials $V(x) = g x^j$, where $j \in \mathbb{R}$. We assume that the first lattice site is placed at $x = x_0$ and define the interferometric phase as $\theta = t\, g x_0^j / \hbar$. Accordingly, the phase imprinted on the kth site is $k^j \theta$. From this, we can easily construct the generator as in Eq. (6), which is equal to

$$\hat{h}_j = \sum_{k=1}^{j} k^j \hat{n}_k. \tag{18}$$

The QFI can be again bounded by Eq. (9), giving

$$\Delta^2 \theta \geqslant \frac{1}{m} \frac{1}{(\lambda_{\max} - \lambda_{\min})^2}. \tag{19}$$

The extreme eigenvalues for $j > 0$ are equal to $\lambda_{\min} = N$ for $|\psi_{\min}\rangle$ and $\lambda_{\max} = M^j N$ for $|\psi_{\max}\rangle$, while for $j < 0$ the minimal and maximal eigenvalues are exchanged. The states $|\psi_{\min}\rangle$ and $|\psi_{\max}\rangle$ are still the ones defined in Eq. (10). The best possible sensitivity is thus

$$\Delta^2 \theta \geqslant \frac{1}{m} \frac{1}{(M^j - 1)^2} \frac{1}{N^2}. \tag{20}$$
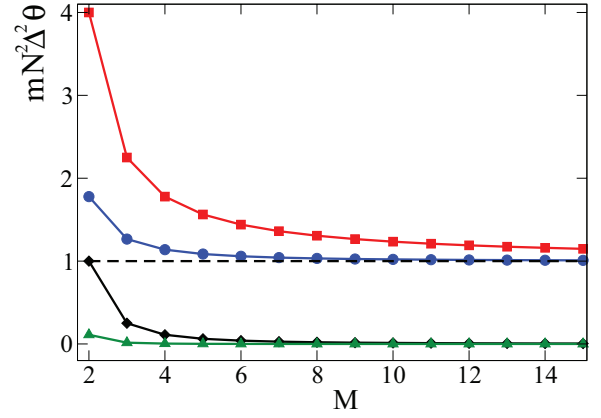

FIG. 1. (Color online) Ultimate scaling of the sensitivity for various nonlinear potentials given by Eq. (20). Red squares, blue circles, black diamonds and green triangles correspond to $j = -2$, $-1, 1, 2$, respectively. The black dashed line denotes the sensitivity of a standard $j = 1, M = 2$ two-mode interferometer.

The behavior with M of the right-hand side of the above equation for various j is shown in Fig. 1. When $j > 0$, $\Delta^2 \theta$ continuously improves with increasing M, and the larger j is, the quicker the improvement is. This would be the case, for instance, for the quadratic potential, i.e., $j = 2$. On the other hand, when the potential decays with distance $j < 0$, as is the case of Casimir-Polder-type interactions, which can exhibit the $j = -3$ or $j = -4$ scaling [39,40], there is no substantial gain from the multimode structure of the interferometer. This happens because the phase imprinted on the second well, which is equal to $2^{-|j|}\theta$, is already negligible when compared to θ. In this case $\Delta^2 \theta \geqslant \frac{1}{m}\frac{1}{N^2}$, and by increasing M the sensitivity saturates to the value corresponding to a linear potential and two wells since, effectively, only the first well experiences the action of the perturbing potential.

Apart from the ultimate scaling, it is interesting to derive an expression for the sensitivity for symmetric states, as was done in Sec. III B for linear potentials. The derivation does not change substantially with respect to the line of reasoning presented in Appendix A, with the only difference being that the summations over the sites involve k^j instead of k. The resulting sensitivity bound for symmetric states reads

$$\Delta^2 \theta \geqslant \frac{1}{m} \frac{1}{f(N)} \frac{M^2}{4\big[M H_M^{(-2j)} - \big(H_M^{(-j)}\big)^2\big]}, \tag{21}$$

where $H_n^{(r)} = \sum_{k=1}^{n} k^{-r}$ is known as the Harmonic number. For $j > 0$ and a large number of lattice sites, the sensitivity bound can be approximated by

$$\Delta^2 \theta \geqslant \frac{1}{m} \frac{1}{f(N)} \frac{1}{M^{2j}} \frac{(1+j)^2(1+2j)}{(2j)^2}, \tag{22}$$

which shows that the M^{-j} improvement on $\Delta \theta$ is preserved for symmetric states.

We underscore that, via Eq. (20), the multimode interferometer could serve as a sensitive tool to determine the spatial dependence of the perturbing potential. This could be experimentally achieved by estimating the phase with various numbers of sites and finding the scaling of $\Delta \theta$ with M. This is an important point, for instance, in the context of the

determination of the Casimir-Polder force or deviations from Newton's law of gravity at the micrometer scale.

IV. SENSITIVITY FOR THE FIT TO THE INTERFERENCE PATTERN

The QFI was used above to set the lower limit for the sensitivity by optimizing $\Delta^2\theta$ with respect to the output measurement and estimator. Below we demonstrate that the scaling of the sensitivity with M, which is present in Eq. (17), is preserved even for a particularly simple phase estimation protocol, although the sensitivity does not saturate the QFI. Also the scaling with N is preserved for the superfluid and phase-squeezed states.

We assume that, after the system acquires the phase as in Eq. (5), the optical lattice is switched off and the wave-packets $\psi_k(x)$, which were initially localized at each site, expand and in the far field form an interference pattern. Positions of atoms are recorded, and the phase is estimated by fitting the density $\rho(x|\theta) = \langle \hat{\Psi}^\dagger(x|\theta)\hat{\Psi}(x|\theta) \rangle$ to the acquired data. In our past work [35] we have shown that when this estimation protocol is employed, the sensitivity is given by

$$\Delta^2\theta = \frac{1}{m}\frac{F_1 + C}{F_1^2}, \tag{23}$$

where F_1 is the one-body Fisher information, which reads

$$F_1 = \int dx \frac{1}{\rho(x|\theta)}\left(\frac{\partial\rho(x|\theta)}{\partial\theta}\right)^2. \tag{24}$$

The coefficient C depends on both the one- and two-body correlations,

$$C = \int dx \int dy\, G^{(2)}(x,y|\theta)\,\partial_\theta \ln\left[\rho(x|\theta)\right]\,\partial_\theta \ln\left[\rho(y|\theta)\right], \tag{25}$$

where $G^{(2)}(x,y|\theta) = \langle\hat{\Psi}^\dagger(x|\theta)\hat{\Psi}^\dagger(y|\theta)\hat{\Psi}(y|\theta)\hat{\Psi}(x|\theta)\rangle$. Our goal is to analyze how the sensitivity (23) depends on both the number of sites M and the nonclassical correlations present in state (2).

In Sec. III B we have seen that the usefully entangled states for the present interferometer have enhanced number fluctuations. In particular, the NOON state provides the best scaling with the number of particles N. This statement, however, assumes that we are always able to perform the optimal measurement, which, in general, depends itself on the input state. In this section, instead, we fix the measurement (as described above) and study the behavior of the sensitivity for different states characterized by enhanced number fluctuations (we will see that such states are still the useful ones for the particular measurement considered). For two lattice sites ($M = 2$), one can easily generate a family of such usefully entangled states by numerically finding the ground state of the two-well Bose-Hubbard Hamiltonian,

$$\hat{H}_{\text{BH}} = -E_J \hat{J}_x + U \hat{J}_z^2, \tag{26}$$

with $U < 0$. Here, E_J is the Josephson energy, related to the frequency of the interwell tunneling, and U is the amplitude of the on-site two-body interactions. This procedure for generating the input states is also relevant for the setup we consider since it will correspond to adiabatical preparation

in the lattice. Performing an analogous calculation for higher M is very demanding since the dimensionality of the Hilbert space grows rapidly, as indicated by the multiple sums present in Eq. (1). This difficulty can be overcome by replacing the true state (1) with

$$|\psi\rangle = \bigotimes_{k=1}^{M}\sum_{n_k=0}^{\infty} C_{n_k}|n_k\rangle. \tag{27}$$

This is the Gutzwiller approximation of the quantum state of the bosons (see [32] and references therein). The number of atoms is not fixed anymore, but in analogy to the fixed-N case (2), we assume that the average number of atoms per site is $\langle\hat{n}_k\rangle = \frac{N}{M}$, so that the average number of atoms in the whole system is N.

Note that although such a state does not recover correlations among the wells, it can be used to mimic nonclassical correlations by increasing the *on-site* atom number variance $\Delta^2\hat{n}$. This is because interferometry employs *particle*, rather than the *mode*, entanglement to improve the precision $\Delta\theta$. For instance, when the MZI is fed with a twin-Fock state $|\frac{N}{2}\rangle \otimes |\frac{N}{2}\rangle$, a product of $\frac{N}{2}$ particles in two modes, it gives the sensitivity close to the HL. This is because the particles, contrary to the modes, are extremely entangled, which can be seen by using the language of the "first quantization," where the state is symmetrized upon the interchange of any two particles.

In order to calculate the sensitivity (23), we express the field operator $\hat{\Psi}(x|\theta)$ in the far field,

$$\hat{\Psi}(x|\theta) = \tilde{\psi}\left(\frac{x}{\tilde{\sigma}^2}\right)\sum_{k=1}^{M} e^{-i\phi(x)\cdot k}\hat{a}_k. \tag{28}$$

We assumed that, initially, all the wave packets $\psi_k(x)$ had identical shapes but were localized around separated sites of the optical lattice. The function $\tilde{\psi}$ is the Fourier transform of $\psi_k(x)$, which is common for each well, and $\tilde{\sigma} = \sqrt{\frac{\hbar t}{\mu}}$ (μ is the atomic mass, and t is the expansion time). The phase factor is defined as

$$\phi(x) = 2\frac{x_0}{\tilde{\sigma}^2}x + \theta, \tag{29}$$

where x_0 is the lattice spacing first introduced below Eq. (4).

The density $\rho(x|\theta)$ obtained using Eqs. (27) and (28) is

$$\rho(x|\theta) = \langle\psi|\hat{\Psi}^\dagger(x|\theta)\hat{\Psi}(x|\theta)|\psi\rangle = N\left|\tilde{\psi}\left(\frac{x}{\tilde{\sigma}^2}\right)\right|^2 s(x|\theta), \tag{30}$$

where $|\tilde{\psi}|^2$ is the envelope of the interference pattern, while the fringes are contained in

$$s(x|\theta) = 1 + \frac{\langle\hat{a}\rangle^2}{N}\left(\frac{\sin^2\left(\frac{M\phi(x)}{2}\right)}{\sin^2\left(\frac{\phi(x)}{2}\right)} - M\right). \tag{31}$$

Expression (30) is put into Eq. (24), giving

$$F_1 = N \int dx \left|\tilde{\psi}\left(\frac{x}{\tilde{\sigma}^2}\right)\right|^2 \frac{1}{s(x|\theta)}\left(\frac{\partial s(x|\theta)}{\partial\theta}\right)^2. \tag{32}$$

When the density of the interference pattern consists of many fringes, the envelope $|\tilde{\psi}|^2$ varies much slower in x than the function $s(x|\theta)$. An integral of a slowly varying envelope with a

quickly oscillating periodic function can be split into a product of an integral of the envelope alone times the average value of the quickly changing $s(x|\theta)$. Since the envelope is normalized, we immediately get

$$F_1 = N \int_0^{2\pi} \frac{d\phi}{2\pi} \frac{1}{s(\phi)} \left(\frac{\partial s(\phi)}{\partial \phi} \right)^2, \qquad (33)$$

where ϕ was defined in Eq. (29). This integral depends on the quantum state through the average value $\langle \hat{a} \rangle$, as can be seen from Eq. (30). Apart from the analytical case $M = 2$, its value has to be calculated numerically.

In the next step, we calculate the coefficient C, which depends on the second-order correlation function. After a lengthy calculation we obtain (see Appendix B for details)

$$C = \left[\langle \hat{a}^2 \rangle^2 - \left(\frac{N}{M} \right)^2 + 2\frac{N}{M}\langle \hat{a} \rangle^2 - 2\langle \hat{a}^2 \rangle \langle \hat{a} \rangle^2 \right] I_1$$
$$+ \left[2\langle \hat{a}^2 \rangle \langle \hat{a} \rangle^2 - 2\frac{N}{M}\langle \hat{a} \rangle^2 \right] I_2, \qquad (34)$$

where the two integrals are given by

$$I_1 = \int_{-\pi}^{\pi} \frac{d\phi}{2\pi} \int_{-\pi}^{\pi} \frac{d\phi'}{2\pi} \, \partial_\theta \ln[s(\phi)] \partial_\theta[s(\phi')]$$
$$\times \frac{\cos[M(\phi + \phi')] - 1}{\cos[\phi + \phi'] - 1} \qquad (35)$$

and

$$I_2 = \int_{-\pi}^{\pi} \frac{d\phi}{2\pi} \int_{-\pi}^{\pi} \frac{d\phi'}{2\pi} \, \partial_\theta \ln[s(\phi)] \partial_\theta[s(\phi')]$$
$$\times \frac{\sin\left[\frac{M}{2}\phi\right] \sin\left[\frac{M}{2}\phi'\right] \sin\left[\frac{M}{2}(\phi + \phi')\right]}{\sin\left[\frac{\phi}{2}\right] \sin\left[\frac{\phi'}{2}\right] \sin\left[\frac{\phi+\phi'}{2}\right]}. \qquad (36)$$

As a first test of Eqs. (33) and (34), in the next section we show that for $M = 2$ we recover a known analytical expression for the sensitivity obtained using a two-mode state with fixed N [35,41].

A. Fit sensitivity with two lattice sites

To make a direct comparison, we start by recalling the main result of our previous work [35], where we focused on phase estimation with a fixed-N two-mode state $|\psi\rangle = \sum_{n=0}^{N} C_n |n, N - n\rangle$. In the resulting N-qubit space, every possible interferometric operation can be mapped into a rotation, with the angular momentum operators $\hat{J}_x = \frac{1}{2}(\hat{a}^\dagger \hat{b} + \hat{a}\hat{b}^\dagger)$, $\hat{J}_y = \frac{1}{2i}(\hat{a}^\dagger \hat{b} - \hat{a}\hat{b}^\dagger)$ and $\hat{J}_z = \frac{1}{2}(\hat{a}^\dagger \hat{a} - \hat{b}^\dagger \hat{b})$. We have shown that when the phase is deduced from the fit of the one-body density to the interference pattern formed by two expanding wave packets, the sensitivity (23) can be expressed in terms of two quantities. One is the spin-squeezing parameter [38], which is a measure of entanglement related to the phase squeezing of $|\psi\rangle$ and reads $\xi_\phi = \sqrt{N \frac{\Delta^2 \hat{J}_y}{\langle \hat{J}_x \rangle^2}}$. The other is the visibility of the interference fringes, $\nu = \frac{2}{N}\langle \hat{J}_x \rangle$. The sensitivity

$$\Delta^2 \theta = \frac{1}{mN}\left[\xi_\phi^2 + \frac{\sqrt{1 - \nu^2}}{\nu^2} \right] \qquad (37)$$

results from the interplay between the growing entanglement ($\xi_\phi^2 \to 0$) and the loss of the visibility ($\nu \to 0$). Naturally, there is some optimally squeezed state which gives the minimal value of $\Delta^2 \theta$, as discussed in [35].

We now calculate the sensitivity (23) using the Gutzwiller approximation (27) for two wells and check how it compares with the exact result (37). As shown in Appendix C, in this case, both the one-body Fisher information (33) and the coefficient C [Eq. (34)] can be evaluated analytically, and the outcome is

$$\Delta^2 \theta = \frac{1}{mN}\left[\tilde{\xi}_\phi^2 + \frac{\sqrt{1 - \tilde{\nu}^2}}{\tilde{\nu}^2} \right], \qquad (38)$$

where the tilde sign denotes the phase-squeezing parameter and the visibility calculated with a product state. Although Eqs. (37) and (38) have identical forms, we still have to verify whether the two-well entanglement of the fixed-N state can be reproduced with a product state by increasing the on-site fluctuations. We model the coefficients of Eq. (27) with a Gaussian,

$$C_{n_k} \propto e^{-\frac{(n_k - \langle n \rangle)^2}{2\sigma^2}}, \qquad (39)$$

where $\langle n \rangle = \frac{N}{2}$ for a two-mode state. The on-site atom number variance is simply $\Delta^2 \hat{n} = \sigma^2$; thus a coherent superfluid state can be modeled by setting the fluctuations at the Poissonian level, i.e., $\sigma = \sqrt{N}$. To check if Eq. (38) will drop below the SNL when the fluctuations are super-Poissonian, we proceed as follows. For various values of $\sigma > \sqrt{N}$ we calculate the phase-squeezing parameter $\tilde{\xi}_\phi^2$ and the visibility $\tilde{\nu}$ and plot the sensitivity (38) as a function of $\tilde{\xi}_\phi^2$. To compare with the fixed-N case, we find the ground state of the Hamiltonian (26) for various values of the ratio $\frac{E_J}{U} < 0$. For every state found in this way, we calculate the phase-squeezing parameter ξ_ϕ^2 and the visibility ν and on the same plot draw the sensitivity (37) as a function of ξ_ϕ^2. Figure 2 shows that not only do Eqs. (38) and (37) have identical forms, but also the quantum correlations
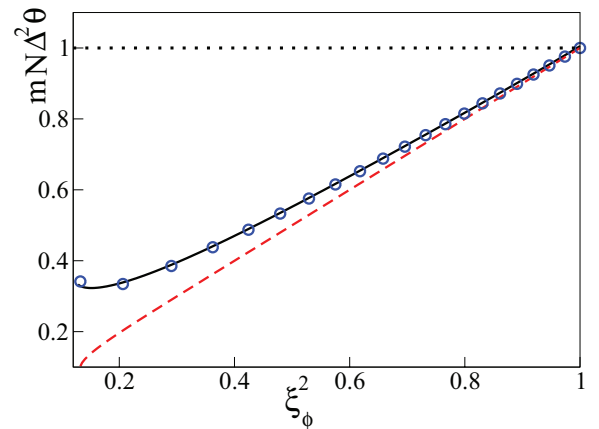

FIG. 2. (Color online) The sensitivity $mN\Delta^2\theta$ of the parameter estimation from the fit to the density of the interference pattern with $M = 2$ and $N = 200$ calculated using the state with a fixed [open blue circles; Eq. (37)] and an unfixed number of atoms [solid black line; Eq. (38)] as a function of the phase-squeezing parameter. The sensitivities shown are normalized to the SNL. The dashed red line shows the ultimate precision of the phase estimation given by the QFI from Eq. (15). The horizontal black dotted line shows the shot-noise limit.

giving sub-shot-noise sensitivity can be perfectly mimicked using a product state [Eq. (27)] with large on-site atom number fluctuations. In both cases, the sensitivity has an optimal point, where the entanglement is balanced by the fringe visibility. Clearly, the Gutzwiller approximation gets worse when the correlations between different wells increase (that is, going farther to the left in Fig. 2), but for the states we consider and this particular measurement, it is precise enough for all practical purposes. Having proven its usefulness, in the following section we employ the Gutzwiller ansatz (27) plus the Gaussian approximation on the coefficient of the product state (39) in order to analyze how the sensitivity (23) behaves for higher M, where results from a fixed-N model are unavailable.

B. Fit sensitivity with M lattice sites

For $M > 2$, when the integrals (33), (35), and (36) cannot be evaluated analytically, we calculate the sensitivity (23) numerically. We fix the average total number of atoms to be $\langle \hat{N} \rangle = 5 \times 10^4$ and for a given M evaluate the sensitivity (23) for different values of the on-site atom number fluctuations using the Gaussian model (39) with $\langle \hat{n} \rangle = \frac{\langle \hat{N} \rangle}{M}$. In order to compare the results for different M, we normalize the sensitivity by the factor $\frac{1}{3}(M^2 - 1)$, that is, by the sensitivity achieved with the best possible measurement, Eq. (17), at the shot-noise level. In Fig. 3 we plot $m\langle \hat{N} \rangle \times \frac{1}{3}(M^2 - 1)\Delta^2\theta$ for $M = 2, 4, 6, 8, 10$, and 12. The outcome is, with a high level of accuracy, independent of M. We thus conclude that the sensitivity of the fit has a form similar to (17), i.e.,

$$\Delta^2\theta = \frac{1}{m} \frac{1}{\zeta(\langle \hat{N} \rangle)} \frac{3}{(M^2 - 1)}, \tag{40}$$

where $\zeta(\langle \hat{N} \rangle)$ is some function of the average total number of atoms, which becomes larger for states with increased on-site atom number fluctuations, $\zeta > \langle \hat{N} \rangle$.
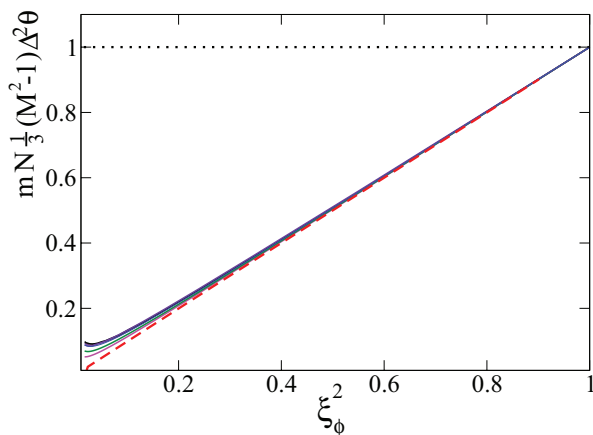

FIG. 3. (Color online) The sensitivity $mN\Delta^2\theta$ of the parameter estimation from the fit to the density of the interference pattern for $M = 2, 4, 6, 8, 10$, and 12 (different colored solid lines) with a fixed average number of atoms equal to $\langle \hat{N} \rangle = 5 \times 10^4$. The sensitivities shown are normalized to the SNL and multiplied by the factor $\frac{1}{3}(M^2 - 1)$. The dashed red line shows the ultimate precision of the phase estimation given by the QFI from Eq. (15). The horizontal black dotted line shows the shot-noise limit.

In Fig. 3, as the phase-squeezing parameter drops, the discrepancy between the curves calculated for different M grows. This is a spurious result of the Gutzwiller approximation (27) for the state $|\psi\rangle$. When the average number of atoms in the system is fixed and M is changed, the average on-site occupation varies. This is not a problem as long as the width σ of the Gaussian (39) is small compared to $\langle \hat{n} \rangle$. However, we increase σ to mimic the growing entanglement in the system. Once σ is comparable to $\langle \hat{n} \rangle$, the change in the on-site population for different M becomes relevant. Therefore, by changing M we are actually changing the nature of the quantum state, and in particular, we cannot assume that the squeezing parameter remains fixed. One could avoid this problem by, rather than fixing $\langle \hat{N} \rangle$, fixing the on-site population $\langle \hat{n} \rangle$ and increasing the number of wells so that $\langle \hat{N} \rangle = M\langle \hat{n} \rangle$.

V. CONCLUSIONS

We have analyzed the performance of ultracold bosons trapped inside an optical lattice as an interferometric device for the measurement of spatially dependent forces. For potentials $V(x) = gx^j$ we showed that, optimizing over all possible output measurements, the coupling constant g can be measured with an uncertainty Δg scaling like M^{-j} for a large number of lattice sites M and independent of the quantum state employed. We then showed that this scaling with the number of lattice sites can still be reached with a particular output measurement which is commonly employed with ultracold atoms: a least-squares fit to the interference pattern resulting from the overlap of freely expanding atoms released from the confining potential. In order to achieve the M^{-j} scaling, no quantum correlations are needed, and thus the superfluid state of the atoms in the lattice would allow us to test the improvement of the sensitivity with an increasing number of sites. This state is commonly prepared using ultracold atoms in optical lattices [32]. We also derived the improvements coming from entangling the quantum state. In particular, we consider the SSN scaling with the number of particles N achieved with phase-squeezed states. Such states could, for instance, be prepared as the ground states of the ultracold atoms in the optical lattice in the presence of a negative contact interaction.

The device here studied is an example of a matter-wave multipath interferometer. While the sensitivity bounds for a general two-path interferometer have already largely been studied, the same analysis based on rigorous estimation theory results has not yet been performed for multipath devices. Moreover, the potential of the implementation of these devices with atoms seems very promising due to the growing control and tunability of the available trapping and probing tools, especially for ultracold atoms.

Finally, we underscore that the precision of the time-of-flight interferometer, where the phase is estimated from the fit of the averaged density to the measured interference pattern, cannot be surpassed by adding a hopping term to the generating Hamiltonian (4). The presence of the hopping, which induces the Bloch oscillations, is an extra complication, which changes the optimal states depending on the ratio between the tunneling energy to the phase related energy ϵ but does not introduce any further benefit. Some of these conclusions can be found in [40] and will be discussed in detail elsewhere.

APPENDIX A: CALCULATION OF THE QFI

In order to calculate the F_Q, we need to derive an expression for the variance of the operator $\hat{h}$. Using definition (6), we get

$$\langle \hat{h}^2 \rangle = \sum_{k_1, k_2} k_1 k_2 \langle \hat{n}_{k_1} \hat{n}_{k_2} \rangle = \sum_k k^2 \langle \hat{n}_k^2 \rangle + \sum_{k_1 \neq k_2} k_1 k_2 \langle \hat{n}_{k_1} \hat{n}_{k_2} \rangle. \tag{A1}$$

We now make use of the symmetry between the wells. The average value $\langle \hat{n}_k^2 \rangle$ does not depend on index k and thus can be denoted as $\langle \hat{n}^2 \rangle$. The same argument concerns the interwell correlation $\langle \hat{n}_{k_1} \hat{n}_{k_2} \rangle$, which will be denoted as $\langle \hat{n}_i \hat{n}_j \rangle$, where i,j are indices of *any* two sites. The above expression thus boils down to

$$\langle \hat{h}^2 \rangle = \langle n^2 \rangle \sum_k k^2 + \langle \hat{n}_i \hat{n}_j \rangle \sum_{k_1 \neq k_2} k_1 k_2$$

$$= \frac{M}{6}(M+1)(2M+1)\langle \hat{n}^2 \rangle$$

$$+ \langle \hat{n}_i \hat{n}_j \rangle \frac{M}{12}(M^2 - 1)(3M + 2). \tag{A2}$$

Our next step is to show that $\langle \hat{n}_i \hat{n}_j \rangle$ can be written as a function of $\langle \hat{n}^2 \rangle$ only. To this end, since the state is symmetric, we can take $i = 1$ and $j = M$ and obtain

$$\langle \hat{n}_1 \hat{n}_M \rangle = \sum_{\vec{n}} C_{\vec{n}}^2 \, n_1 (N - n_1 - \cdots - n_{M-1}) \tag{A3}$$

$$= \frac{N^2}{M} - \sum_{\vec{n}} C_{\vec{n}}^2 \, n_1 (n_1 + \cdots + n_{M-1}). \tag{A4}$$

Now, since it does not matter which two wells we correlate, in the sum, instead of n_1, we can use an average over $M - 1$ wells as follows:

$$\langle \hat{n}_1 \hat{n}_2 \rangle = \frac{N^2}{M} - \sum_{\vec{n}} C_{\vec{n}}^2 \, \frac{n_1 + \cdots + n_{M-1}}{M - 1}(n_1 + \cdots + n_{M-1}). \tag{A5}$$

Finally, we exploit the fact that the total number of atoms is fixed and thus $n_1 + \cdots + n_{M-1} = N - n_M$ and obtain

$$\langle \hat{n}_1 \hat{n}_M \rangle = \frac{N^2}{M} - \sum_{\vec{n}} C_{\vec{n}}^2 \, \frac{(N - n_M)^2}{M - 1} \tag{A6}$$

$$= \frac{N^2}{M} - \frac{\langle n^2 \rangle - 2N^2/M + N^2}{M - 1}. \tag{A7}$$

Using the result for the average value of $\hat{h}$, we finally obtain

$$F_Q = 4\Delta^2 \hat{h} = \tfrac{1}{3}(M+1)M^2 \Delta^2 \hat{n}, \tag{A8}$$

where $\Delta^2 \hat{n} = \langle \hat{n}^2 \rangle - \langle \hat{n} \rangle^2$ is the on-site variance.

APPENDIX B: CALCULATION OF THE SENSITIVITY

In this appendix we give details of the derivation of coefficient C from Eq. (34), which is used to evaluate the sensitivity (23) using the product state (27). In order to calculate C, one first has to find the second-order correlation function,

$$G^{(2)}(x,y|\theta) = \langle \hat{\Psi}^\dagger(x|\theta)\hat{\Psi}^\dagger(y|\theta)\hat{\Psi}(y|\theta)\hat{\Psi}(x|\theta) \rangle. \tag{B1}$$

When the field operator, which is introduced in Eq. (28), is put into this definition, we obtain

$$G^{(2)}(x,y|\theta) = \left| \tilde{\psi}\left(\frac{x}{\tilde{\sigma}^2}\right) \right|^2 \left| \tilde{\psi}\left(\frac{y}{\tilde{\sigma}^2}\right) \right|^2 \sum_{k_1,k_2,k_3,k_4=1}^{M} e^{i\phi(x)(k_1 - k_4)}$$

$$\times e^{i\phi(y)(k_2 - k_3)} \langle \hat{a}_{k_1}^\dagger \hat{a}_{k_2}^\dagger \hat{a}_{k_3} \hat{a}_{k_4} \rangle, \tag{B2}$$

where $\phi(x) = 2\frac{x_0}{\tilde{\sigma}^2}x + \theta$. The above sum cannot be performed in a straightforward manner since special care has to be taken to distinguish cases when the indices $k_1 \cdots k_4$ in the average value $\langle \hat{a}_{k_1}^\dagger \hat{a}_{k_2}^\dagger \hat{a}_{k_3} \hat{a}_{k_4} \rangle$ are equal to or different from each other. A careful classification of all the possible terms gives

$$G^{(2)}(x,y|\theta) = \left| \tilde{\psi}\left(\frac{x}{\tilde{\sigma}^2}\right) \right|^2 \left| \tilde{\psi}\left(\frac{y}{\tilde{\sigma}^2}\right) \right|^2 \times \{ M\langle \hat{a}^\dagger \hat{a}^\dagger \hat{a}\hat{a} \rangle + (s(x+y) - M)\langle \hat{a}^\dagger \hat{a}^\dagger \rangle^2 + \langle \hat{n} \rangle^2 (s(x-y) + M^2)$$

$$+ 2[s(x) + s(y) - 2M]\langle \hat{a}^\dagger \hat{a}^\dagger \hat{a} \rangle \langle \hat{a} \rangle + \langle \hat{n} \rangle \langle \hat{a} \rangle^2 [8M - 2M^2 + (M-4)(s(x) + s(y)) - 2s(x-y) + 2g(x,-y)]$$

$$+ \langle \hat{a} \rangle^2 \langle \hat{a}^2 \rangle [4M - 2s(x) - 2s(y) - 2s(x+y) + 2g(x,y)] + \langle \hat{a} \rangle^4 [s(x)s(y) - (M-4)(s(x) + s(y)) + s(x+y)$$

$$+ s(x-y) - 2g(x,y) - 2g(x,-y) + M^2 - 6M]\}. \tag{B3}$$

The function $s(x)$ is defined as

$$s(x) = \frac{\cos[M\phi(x)] - 1}{\cos[\phi(x)] - 1}, \tag{B4}$$

while the $g(x,y)$ function is

$$g(x,y) = \frac{\sin\left[\frac{M\phi(x)}{2}\right] \sin\left[\frac{M\phi(y)}{2}\right] \sin\left[\frac{M(\phi(x)+\phi(y))}{2}\right]}{\sin\left[\frac{\phi(x)}{2}\right] \sin\left[\frac{\phi(y)}{2}\right] \sin\left[\frac{\phi(x)+\phi(y)}{2}\right]}. \tag{B5}$$

The coefficient C is defined as a double integral of the above second-order correlation function with the one-body probabilities calculated at positions x and y, namely,

$$C = \int dx \int dy\, G^{(2)}(x,y|\theta) \partial_\theta \ln[\rho(x|\theta)]\, \partial_\theta \ln[\rho(y|\theta)]. \tag{B6}$$

The one-body density is defined in Eq. (30). We use the fact that the interference pattern consists of many fringes, so that the envelope $|\tilde{\psi}|^2$ varies slowly compared to the oscillatory functions present in s, g, and the density ρ. Therefore, the integral (B6) can be rewritten as

$$C = \int_{-\pi}^{\pi} \frac{d\phi}{2\pi} \int_{-\pi}^{\pi} \frac{d\phi'}{2\pi}\, G^{(2)}(\phi,\phi'|\theta)$$
$$\times\, \partial_\theta \ln[\rho(\phi|\theta)]\, \partial_\theta \ln[\rho(\phi'|\theta)], \tag{B7}$$

where we changed the variables $x \to \phi$ and $y \to \phi'$. It can be demonstrated that

$$\int_{-\pi}^{\pi} \frac{d\phi}{2\pi} \partial_\theta \ln[\rho(\phi|\theta)] = 0; \tag{B8}$$

therefore all the terms from Eq. (B3) which do not depend on both ϕ and ϕ' are zero. Using a property of the functions f and g,

$$\int_{-\pi}^{\pi} \frac{d\phi}{2\pi} \int_{-\pi}^{\pi} \frac{d\phi'}{2\pi} s(\phi+\phi')\partial_\theta \ln[\rho(\phi|\theta)]\, \partial_\theta \ln[\rho(\phi'|\theta)]$$
$$= -\int_{-\pi}^{\pi} \frac{d\phi}{2\pi} \int_{-\pi}^{\pi} \frac{d\phi'}{2\pi} s(\phi-\phi')\partial_\theta$$
$$\times\, \ln[\rho(\phi|\theta)]\, \partial_\theta \ln[\rho(\phi'|\theta)],$$

and the same with $g(\phi,\phi')$ and $g(\phi,-\phi')$, we finally get

$$C = [\langle \hat{a}^2 \rangle^2 - \langle \hat{n} \rangle^2 + 2\langle \hat{n} \rangle \langle \hat{a} \rangle^2 - 2\langle \hat{a}^2 \rangle \langle \hat{a} \rangle^2]$$
$$\times \int_{-\pi}^{\pi} \frac{d\phi}{2\pi} \int_{-\pi}^{\pi} \frac{d\phi'}{2\pi}\, \partial_\theta \ln[s(\phi)]\partial_\theta[s(\phi')]s(\phi+\phi')$$
$$+ [2\langle \hat{a}^2 \rangle \langle \hat{a} \rangle^2 - N\langle \hat{a} \rangle^2]$$
$$\times \int_{-\pi}^{\pi} \frac{d\phi}{2\pi} \int_{-\pi}^{\pi} \frac{d\phi'}{2\pi}\, \partial_\theta \ln[s(\phi)]\partial_\theta[s(\phi')]g(\phi,\phi'),$$

which coincides with Eq. (34).

APPENDIX C: SENSITIVITY FOR TWO WELLS

First, we calculate the one-body Fisher information defined in Eq. (33). For $M = 2$ the s function from Eq. (31) reads

$$s(\phi) = 1 + \tilde{\nu} \cos\phi, \tag{C1}$$

where $\tilde{\nu}$ is the fringe visibility calculated with a product state,

$$\tilde{\nu} = \frac{2}{N} \langle \hat{J}_x \rangle = \frac{2}{N} \frac{\langle \hat{a}^\dagger \rangle \langle \hat{b} \rangle + \langle \hat{a} \rangle \langle \hat{b}^\dagger \rangle}{2} = \frac{2}{N} \langle \hat{a} \rangle^2, \tag{C2}$$

where we used the symmetry between the two wells and the last step was possible because the coefficients C_n are taken to be real. We insert (C1) into (33) and obtain an analytical outcome:

$$F_1 = 1 - \sqrt{1 - \tilde{\nu}^2}. \tag{C3}$$

The integrals I_1 from Eq. (35) and I_2 from Eq. (36) can be calculated in a similar way, giving

$$I_1 = I_2 = \frac{2}{\tilde{\nu}^2}(-2 + \tilde{\nu}^2 + 2\sqrt{1 - \tilde{\nu}^2}). \tag{C4}$$

As a result coefficient C from Eq. (34) for $M = 2$ reads

$$C = \frac{2}{\tilde{\nu}^2}(-2 + \tilde{\nu}^2 + 2\sqrt{1 - \tilde{\nu}^2})\left[\langle \hat{a}^2 \rangle^2 - \frac{N^2}{4}\right]. \tag{C5}$$

Finally, we note that for a symmetric state $\langle \hat{J}_y \rangle = 0$; thus the variance of the $\hat{J}_y$ operator calculated using a product state reads

$$\Delta^2 \hat{J}_y = \frac{1}{2}\left[\frac{N^2}{4} + \frac{N}{2} - \langle \hat{a}^2 \rangle^2\right], \tag{C6}$$

which allows us to rewrite Eq. (C5) in a following way:

$$C = \frac{4}{\tilde{\nu}^2}(-2 + \tilde{\nu}^2 + 2\sqrt{1 - \tilde{\nu}^2})\left[\frac{N}{4} - \tilde{\Delta}^2 \hat{J}_y\right]. \tag{C7}$$

Combining (C3) and (C7) as in Eq. (23), we obtain

$$\Delta^2 \theta = \frac{1}{mN}\left[\tilde{\xi}_\phi^2 + \frac{\sqrt{1 - \tilde{\nu}^2}}{\tilde{\nu}^2}\right], \tag{C8}$$

where $\tilde{\xi}_\phi^2$ is the phase-squeezing parameter calculated with a product state.

[1] For a review see V. Giovanetti, S. Lloyd, and L. Maccone, Science **306**, 1330 (2004).
[2] V. Giovannetti, S. Lloyd, and L. Maccone, Phys. Rev. Lett. **96**, 010401 (2006).
[3] L. Pezzé and A. Smerzi, Phys. Rev. Lett. **102**, 100401 (2009).
[4] A. D. Cronin, J. Schmiedmayer, and D. E. Pritchard, Rev. Mod. Phys. **81**, 1051 (2009).
[5] T. A. Pasquini, Y. Shin, C. Sanner, M. Saba, A. Schirotzek, D. E. Pritchard, and W. Ketterle, Phys. Rev. Lett. **93**, 223201 (2004).
[6] Y. J. Lin, I. Teper, C. Chin, and V. Vuletic, Phys. Rev. Lett. **92**, 050404 (2004).
[7] J. M. Obrecht, R. J. Wild, M. Antezza, L. P. Pitaevskii, S. Stringari, and E. A. Cornell, Phys. Rev. Lett. **98**, 063201 (2007).
[8] B. P. Anderson and M. A. Kasevich, Science **282**, 1686 (1998).
[9] M. Fattori, C. D'Errico, G. Roati, M. Zaccanti, M. Jona-Lasinio, M. Modugno, M. Inguscio, and G. Modugno, Phys. Rev. Lett. **100**, 080405 (2008).
[10] F. Baumgartner, R. J. Sewell, S. Eriksson, I. Llorente-Garcia, J. Dingjan, J. P. Cotter, and E. A. Hinds, Phys. Rev. Lett. **105**, 243003 (2010).
[11] D. Leibfried, M. D. Barrett, T. Schaetz, J. Britton, J. Chiaverini, W. M. Itano, J. D. Jost, C. Langer, and D. J. Wineland, Science **304**, 1476 (2004).
[12] M. H. Schleier-Smith, I. D. Leroux, and V. Vuletić, Phys. Rev. Lett. **104**, 073604 (2010).
[13] J. Estève et al., Nature (London) **455**, 1216 (2008).

[14] M. F. Riedel *et al.*, Nature (London) **464**, 1170 (2010).

[15] C. Gross *et al.*, Nature (London) **464**, 1165 (2010).

[16] B. Lücke *et al.*, Science **11**, 773 (2011).

[17] J. Appel *et al.*, Proc. Natl. Acad. Sci. USA **106**, 10960 (2009).

[18] Z. Chen, J. G. Bohnet, S. R. Sankar, J. Dai, and J. K. Thompson, Phys. Rev. Lett. **106**, 133601 (2011).

[19] F. Zernike, J. Opt. Soc. Am. **40**, 326 (1950).

[20] G. M. D'Ariano and M. G. A. Paris, Phys. Rev. A **55**, 2267 (1997).

[21] B. C. Sanders *et al.*, J. Phys. A **32**, 7791 (1999).

[22] J. Soderholm, G. Bjork, B. Hessmo, S. Inoue, J. Soderholm, G. Bjork, B. Hessmo, and S. Inoue, Phys. Rev. A **67**, 053803 (2003).

[23] A. Vourdas and J. A. Dunningham, Phys. Rev. A **71**, 013809 (2005).

[24] S. Yu and C. H. Oh, Phys. Rev. Lett. **108**, 030402 (2012).

[25] F. Impens, F. Pereira dos Santos, and C. J. Bordé, New. J. Phys **13**, 065024 (2011).

[26] F. Impens and C. J. Bordé, Phys. Rev. A **80**, 031602(R) (2009).

[27] J. Petrovic, I. Herrera, P. Lombardi, and F. S. Cataliotti, arXiv:1111.4321.

[28] N. Poli, F. Y. Wang, M. G. Tarallo, A. Alberti, M. Prevedelli, and G. M. Tino, Phys. Rev. Lett. **106**, 038501 (2011).

[29] M. G. Tarallo, A. Alberti, N. Poli, M. L. Chiofalo, F. Y. Wang, and G. M. Tino, Phys. Rev. A **86**, 033615 (2012).

[30] M. G. Tarallo, N. Poli, F. Y. Wang, and G. M. Tino, arXiv:1210.6829.

[31] C. Gross, J. Esteve, M. K. Oberthaler, A. D. Martin, and J. Ruostekoski, Phys. Rev. A **84**, 011609(R) (2011).

[32] I. Bloch, J. Dalibard, and W. Zwerger, Rev. Mod. Phys. **80**, 885 (2008).

[33] M. Greiner, O. Mandel, T. Esslinger, T. W. Hänsch, and I. Bloch, Nature (London) **415**, 39 (2002).

[34] S. Fölling, F. Gerbier, A. Widera, O. Mandel, T. Gericke, and I. Bloch, Nature (London) **434**, 481 (2005).

[35] J. Chwedeńczuk, P. Hyllus, F. Piazza, and A. Smerzi, New J. Phys. **14**, 093001 (2012).

[36] S. L. Braunstein and C. M. Caves, Phys. Rev. Lett. **72**, 3439 (1994).

[37] M. A. Leung, K. W. Mahmud, and W. P. Reinhardt, Mol. Phys. **110**, 801 (2012).

[38] J. Grond, U. Hohenester, I. Mazets, and J. Schmiedmayer, New J. Phys. **12**, 065036 (2010).

[39] M. Antezza, L. P. Pitaevskii, and S. Stringari, Phys. Rev. A **70**, 053619 (2004).

[40] J. Chwedeńczuk, L. Pezzé, F. Piazza, and A. Smerzi, Phys. Rev. A **82**, 032104 (2010).

[41] C. Lee, Phys. Rev. Lett. **97**, 150402 (2006).